N82 23459

Capillary forces exerted by liquid drops caught between crossed cylinders: A 3-D meniscus problem with free contact line

T. W. Patzek and L. E. Scriven

Department of Chemical Engineering & Materials Science,
University of Minnesota, Minneapolis, Minnesota 55455

Abstract

The Young-Laplace equation is solved for three-dimensional menisci between crossed cylinders, with either the contact line fixed or the contact angle prescribed, by means of the Galerkin/finite element method. Shapes are computed, and with them the practically important quantities: drop volume, wetted area, capillary pressure force, surface tension force, and the total force exerted by the drop on each cylinder.

1. Problem statement

A liquid drop between solid fibers (Fig. 1) constitutes a three-phase system whose thermodynamic description may become quite involved (cf. Huh 1969). However, even without gravity, if the fluid-solid contact line differs from a circle, or two coaxial circles, the drop surface generally forms a three-dimensional meniscus of constant curvature, difficult to approximate from experiment and non-trivial to compute from theory. In large drops, gravity joins surface tension in the molding of shape and the situation becomes even more complex. The surface energy of the system in the absence of gravity is

$$E = \underset{\text{liq/vap}}{\sigma_{LV} S_{LV}} + \underset{\text{liq/sol-sol/vap}}{(\sigma_{LS} - \sigma_{SV})\, S_{LS}} + \underset{\text{sol/vap datum}}{E_0} \quad . \qquad [1]$$

Here the solid surface is rigid and the solid-liquid vapor interactions are described by the constant interfacial tensions σ_{LV}, σ_{LS}, and σ_{SV}.

Equilibrium drop shapes make the surface energy stationary, i.e. $\delta E = 0$ for all perturbations that leave the drop volume fixed, $\delta V = 0$, and *either* the contact line fixed, $\delta \underset{\sim}{x}_{LSV} = \underset{\sim}{0}$, *or* the contact angle unchanged, ($\underset{\sim}{n}_{LV} \cdot \underset{\sim}{n}_S = \cos\beta$, where β is the contact angle). These conditions define a variational problem equivalent to the Young-Laplace equation of capillarity — a normal stress balance — with appropriate boundary conditions at the contact line:

capillary pressure — normal interface perturbation

$$\delta E = \int_{S_{LV}} \left[\frac{p_V - p_L}{\sigma_{LV}} - 2H_{LV}(\underset{\sim}{x}_{LV}) \right] \delta \underset{\sim}{x}_{LV} \cdot \underset{\sim}{n}_{LV}\, dS +$$

interface mean curvature; interface location; unit normal to interface

normal contact line perturbation, parallel to solid surface

$$+ \oint_{L_{LSV}} \left[\underset{\sim}{n}_{LV} \cdot \underset{\sim}{n}_S - \frac{\sigma_{SV} - \sigma_{LS}}{\sigma_{LV}} \right] \delta \underset{\sim}{x}_{LV} \cdot \underset{\sim}{t}_{LSV} \times \underset{\sim}{n}_S\, dL = 0 \qquad [2]$$

unit tangent to contact line; unit normal to solid surface; cosine of contact angle β

Eq. [2] makes plain that the vanishing variation forces the Young-Laplace residual, $2H_{LV} - (p_V - p_L)/\sigma_{LV}$, and likewise the Young-Dupré residual, $\cos\beta - (\sigma_{SV} - \sigma_{LS})/\sigma_{LV}$, to be *orthogonal* (as viewed in the appropriate function space) to admissible normal perturbations.

A drop of liquid trapped between two perpendicular cylinders of equal radii is of interest. When the cylinders touch, their point of contact is taken as the origin (Fig. 2). Spherical coordinates are used to obtain a single-valued representation of the liquid-vapor interface. A sphere of radius R, equal to the cylinder *diameter*, is chosen as the base surface and is centered at the origin.

The unknown position of the interface, measured in the units of R, is

$$\underset{\sim}{x}_{LV} = f(\theta,\phi)\ \underset{\sim}{e}_r \qquad [3]$$

Analogously, the interface perturbation is

$$\delta\underset{\sim}{x}_{LV} = \zeta(\theta,\phi)\ \underset{\sim}{e}_r \qquad [4]$$

Furthermore, in the case of spherical representation, Weingarten's formulas relate the mean curvature of the interface to the divergence of the unit normal on the unit sphere Ω :

$$2H_{LV} = -\frac{1}{f(\theta,\phi)}\,\nabla_\Omega \cdot \underset{\sim}{n}_{LV} \qquad [5]$$

This, together with the divergence theorem, leads to the weak form of Eq. [2]:

$$\int_\Omega \left[-\underset{\sim}{n}_{LV} \cdot (\nabla_\Omega (f\zeta) - 2\zeta\ \underset{\sim}{e}_r) + \frac{P_V - P_L}{\sigma_{LV}}\,\zeta\, f^2 \right] d\Omega \ +$$

(projected domain on unit sphere)

$$+ \oint_\Lambda f\,\zeta\, \underset{\sim}{n}_{LV} \cdot \underset{\sim}{m}_\Omega\, d\Lambda \ +$$

($\underset{\sim}{m}_\Omega$: projected binormal of contact line; Λ: projected contact line)

$$+ \oint_{L_{LSV}} (\underset{\sim}{n}_{LV} \cdot \underset{\sim}{n}_S - \cos\beta)\,\zeta\,\underset{\sim}{e}_r \cdot \underset{\sim}{t}_{LSV} \times \underset{\sim}{n}_S\, dL = 0 \qquad [6]$$

2. Galerkin/finite element method

The main steps of the finite element algorithm can be outlined as follows:

(i) The problem is nonlinear and so an initial estimate of drop shape (*and contact line position*) is needed that falls within the domain of convergence of the iteration method. Estimate from *either* analysis of a limiting case *or* experimental observations *or* a blend of both. The last leads to the inside surface of a *small torus* as an initial guess.

(ii) To discretize the problem, partition the corresponding spherical domain (Fig. 3) into curvilinear quadrilaterals between the equally spaced spines ϕ = constant (cf. Kistler 1981). The spines remain fixed but the nodes of the quadrilaterals can move along them. Let the number of nodes in the partition be N.

(iii) Construct a finite element basis function $\Psi^i(\theta,\phi)$ for the subdomain around each node (cf. Brown, Orr, and Scriven 1979):
- choose the biquadratic polynomial on the (ξ,η)-unit square,
- map each quadrilateral isoparametrically $(\theta,\phi) \to (\xi,\eta)$ onto the unit square. This procedure transforms the original, free boundary domain Ω in (θ,ϕ)-coordinates into a fixed square in the map (ξ,η) (Strang and Fix 1973).

(iv) Approximate the drop shape as

$$f(\theta,\phi) = \sum_1^N \alpha_i\, \Psi^i \left[\theta(\xi,\eta), \phi(\xi,\eta) \right]$$

- nodal values α_i are the coefficients to be found.

(v) Approximate the shape perturbation as

$$\zeta(\theta,\phi) = \sum_{1}^{N} \gamma_i \Psi^i \left[\theta(\xi,\eta),\ \phi(\xi,\eta) \right]$$

- take γ_i as arbitrary coefficients. Because the γ_i's are arbitrary, the Galerkin weighted residuals — to which Eq. [6] transforms under (iv) and (v) — must vanish at equilibrium. This brings out the *direct* link between the *Galerkin* and *variational* approach.

(vi) Solve the resulting N nonlinear algebraic equations for the coefficients α_i using Newton's method.
- update the original domain in each iteration
- use the Jacobian for continuation in the parameter $(p_V - p_L)/\sigma_{LV}$ or V.

(vii) Terminate iteration when the L_∞ norm of residuals, i.e. the largest residual, is smaller than a preset value, e.g. 10^{-6} (as was actually used).

The algorithm was programmed in Fortran and executed on a CDC CYBER-74 computer. It took ca. 2 sec/iteration for 169 unknowns and three to at most five iterations to converge.

A sequence of drop shapes in order of increasing volume is shown in Fig. 4 ($R(p_V - p_L)/\sigma_{LV} \equiv$ LAMBDA). As capillary pressure decreases, the liquid forms drops of increasing volume and finally encircles both cylinders. The plotted drops are stable, including the largest one — the surface of which covers more than half of the cylinder cross-section.

3. Practical quantities

Drops of liquid caught between crossed fibers of non-woven fabrics draw them together by capillary action and, when the liquid solidifies, fasten the fibers together. Similar phenomena occur in paper, where water at times forms droplets by capillary condensation from humid air. Liquid drops between fibers are also present at certain stages of oily soil removal by detergent action. Furthermore, drop behavior between crossed cylinders is important to direct measurement of adhesive forces between solid surfaces in the presence of capillary-condensed liquids (Fisher and Israelachvili 1981). These and other applications call for computation of the following practically important quantities:

(i) drop volume V
(ii) wetted area of each cylinder A
(iii) capillary forces exerted by drop

- capillary pressure force $(p_V - p_L) \int_{S_{LV}} \underline{e}_z \cdot \underline{n}_{LV}\, dS$

- surface tension force $\sigma_{LV} \int_{L_{LSV}} \underline{e}_z \cdot \underline{m}_{LV}\, dL$

- their sum: total force holding crossed cylinders together.

Fig. 5 shows that the total force on the cylinders increases with the wettability of the solid by the liquid. As can be seen from Fig. 6, the components of total force vary widely with the drop volume but their sum increases slowly and approaches an asymptotic limit as the volume shrinks to zero. That limit is $4\pi\sigma_{LV}(R/2)\cos\beta$ (Fisher and Israelachvili 1981), and becomes a good approximation for $R(p_V - p_L)/\sigma_{LV} \sim 10^4$, i.e. for very small drops. If the mean curvature is taken as the independent parameter, the drop volume grows extremely sensitive to it as the contact angle decreases (Fig. 7), whereas the total force again approaches the limit (Fig. 8).

Summary and conclusions

What is described here is an extension of earlier analyses of three-dimensional meniscus shapes (Orr, Brown and Scriven 1977).

Besides yielding equilibrium shapes of drops with *fixed contact lines*, as in past 3-D analyses, the algorithm used here also gives shapes of drops with a *prescribed contact angle*, which is sometimes a closer approximation to reality.

Computations for other cases of 3-D menisci making a prescribed contact angle can be treated similarly. Augmented by a block-Lanczos method for solving the related

eigenproblem (see Brown and Scriven 1980), the algorithm tests stability with respect to admissible perturbations with the contact line fixed. The case of prescribed contact angle is more difficult but is also being treated in the continuation of this work.

The results show that total capillary force between cylinders increases with decreasing contact angle, i.e. with better wetting. Capillary force also increases with *decreasing* drop volume, approaching an asymptotic limit. However, the wetted area on each cylinder decreases with decreasing drop volume, which raises the question of the optimum drop volume to strive for, when permanent bonding is sought from solidified liquid. For then the strength of the bond is likely to depend upon the area of contact, which is the wetted area when the bonding agent was introduced in liquid form.

Acknowledgment

This research was supported by the NASA Fund for Independent Research.

References

R. A. Brown, F. M. Orr Jr., and L. E. Scriven, Three-Dimensional Menisci: Numerical Simulation by Finite Elements, *J. Colloid Interface Sci.* 60 137 (1977).

R. A. Brown, F. M. Orr Jr., and L. E. Scriven, Static Drop on an Inclined Plate: Analysis by the Finite Element Method, *J. Colloid Interface Sci.* 73 76 (1980).

R. A. Brown and L. E. Scriven, The Shapes and Stability of Captive Rotating Drops, *Phil. Trans. Roy. Soc.* 297 51 (1980).

C. Huh, Capillary Hydrodynamics, Interfacial Instability and the Solid/Liquid/Fluid Contact Line, Ph.D. Thesis, University of Minnesota (1969).

L. R. Fisher and J. N. Israelachvili, Direct Measurement of the Effect of Meniscus Forces on Adhesion . . ., *J. Colloid Interface Sci.* submitted (1981).

L. R. Fisher and J. N. Israelachvili, Experimental Studies on the Applicability of the Kelvin Equation to Highly Curved Nonlinear Menisci, *J. Colloid Interface Sci.* submitted (1981).

S. F. Kistler, First International Fluid Mechanics Winter (Summer) Seminar, INTEC - Santa Fe, 18-21 August 1981.

G. Strang and G. J. Fix, *An Analysis of the Finite Element Method*, Prentice-Hall, Inc., Englewood Cliffs, N. J. (1973).

Fig. 1. Liquid drop caught between crossed cylinders

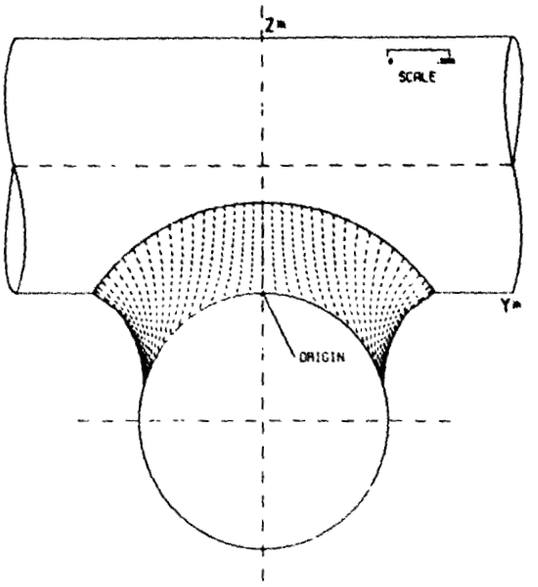

Fig. 2
Two cylinders of equal radii crossed
at right angle — coordinate system

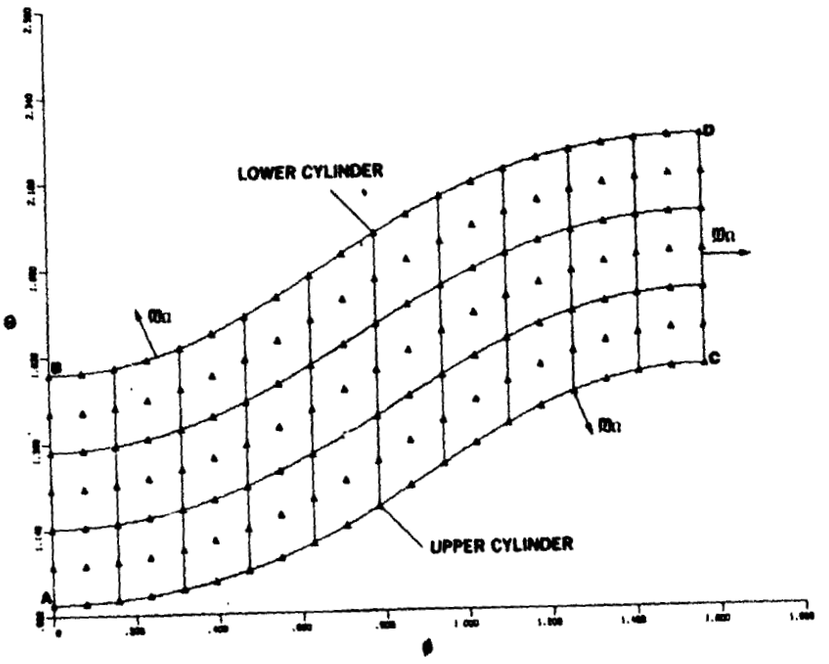

Fig. 3
Typical computational domain in spherical coordinates

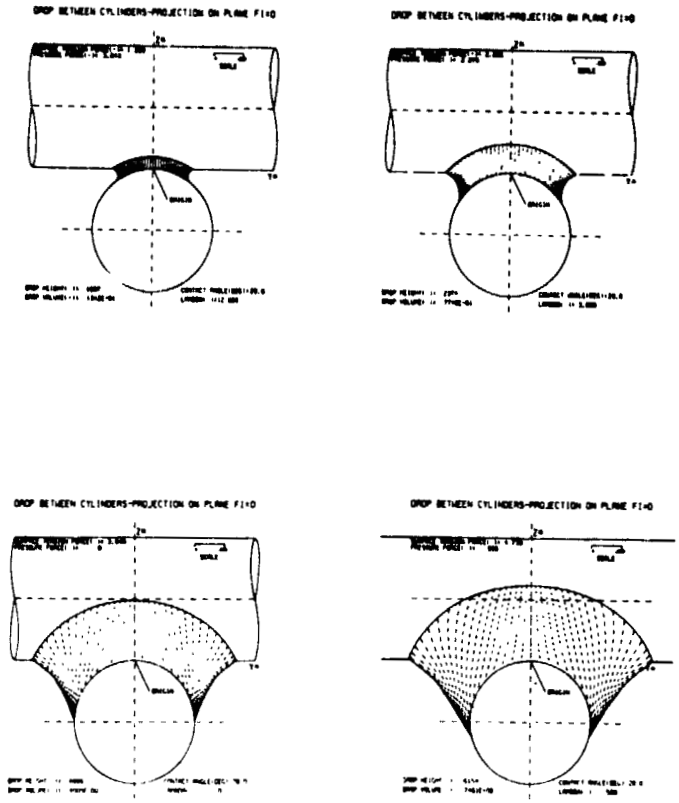

Fig. 4

Sequence of drop shapes in order of increasing volume.
Dimensionless capillary pressure $R(p_V - p_L)/\sigma_{LV}$ = LAMBDA.

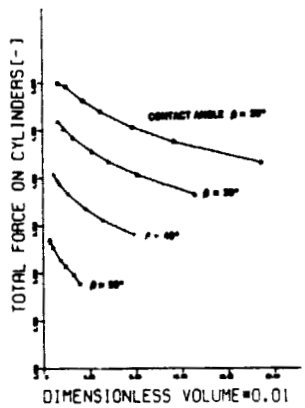

Fig. 5

Total force exerted by drop
on each cylinder vs. drop volume.

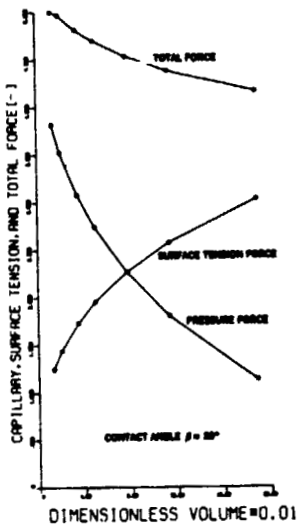

Fig. 6

Components of the total force
vs. drop volume.

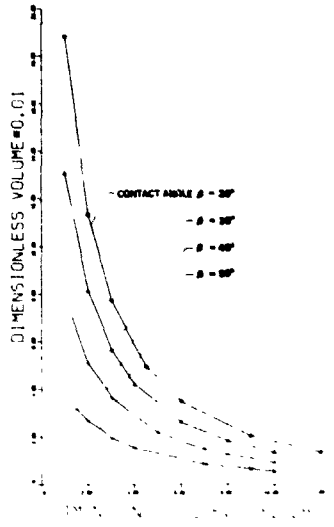

Fig. 7
Drop volume vs.
capillary pressure

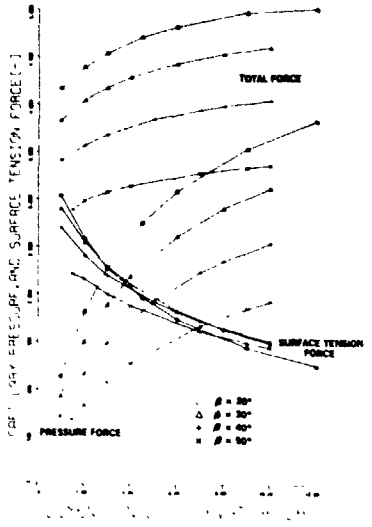

Fig. 8
Forces exerted by
drop on each cylinder
vs. capillary pressure

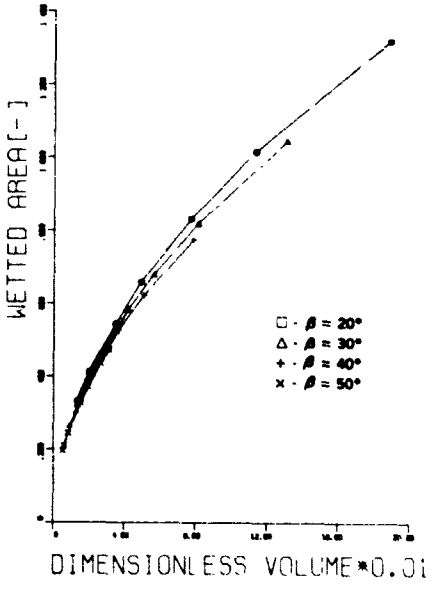

Fig. 9
Wetted area on each cylinder vs. drop volume